Predicting Creep Failure from Cracks in a Heterogeneous Material using Acoustic Emission and Speckle Imaging

Leevi Viitanen,[1] Markus Ovaska,[1] Sumit Kumar Ram,[1] Mikko J. Alava,[1,*] and Pasi Karppinen[2]

[1] *COMP Center of Excellence, Department of Applied Physics, Aalto University School of Science, P.O.Box 11100, FI-00076 AALTO, Espoo, Finland;*

[2] *ProtoRhino Ltd, Betonimiehenkuja 5 C, FI-02150 Espoo, Finland*

(Received 11 December 2017; revised manuscript received 6 June 2018; published 6 February 2019)

Finding out when cracks become unstable is at the heart of fracture mechanics. Cracks often grow by avalanches and when a sample fails depends on its past avalanche history. We study the prediction of sample failure in creep fracture under a constant applied stress and induced by initial flaws. Individual samples exhibit fluctuations around a typical rheological response or creep curve. Predictions using the acoustic emission from the intermittent crack growth are not feasible until well beyond the sample-dependent minimum strain rate. Using an optical speckle analysis technique, we show that predictability is possible later because of the growth of the fracture process zone.

DOI: 10.1103/PhysRevApplied.11.024014

I. INTRODUCTION

To predict the failure of a sample seems easy at first: establish the limiting strength of the material at hand and measure the loads it is subjected to. When the ultimate strength limit is exceeded the sample will fail. However, this is not so easy for two fundamental reasons. Even in simpler brittle materials the size effects of fracture strength are complicated and can at best be understood in the statistical sense using extremal statistics. More generally, the past deformation history is of importance because the sample has complicated internal stresses, the microstructure evolves, damage accumulates, or a dominant stable microcrack grows.

Here, we consider creep loading of material samples with pre-existing defects as a life-time prediction problem in statistical fracture. The topic of failure prediction is of considerable interest as a fundamental problem in the physics of fracture, and is also an old one in such applications as the monitoring of large-scale structures (buildings) and following the behavior of machinery components. The crackling noises or fracture avalanches [1,2] are important since they indicate that fracture mechanics needs to be understood by the tools of critical phenomena [3], just as for other intermittent processes such as fluid invasion of porous media, plastic deformation, or dynamics of domain walls in many condensed matter examples. The intermittent advance of single cracks and the related crack-front roughness and avalanches are important. Sometimes the behavior can even be quantitatively matched with predictions following from a nonequilibrium depinning transition of the crack as a front in a disordered medium with long-range elasticity [1,4–6]. Creep is an example of a class of deformation problems from earthquakes [7–16] to laboratory-scale fractures, for which one wants to try lifetime or catastrophic-event prediction [17–33].

The creep failure of a sample follows from the accelerating growth of a crack and can be summarized on a case-by-case level by empirical growth laws, in analogy to the Paris' law in fatigue fracture. The idea is to write down a growth rate for the crack in a given stress state and with a material parameter that would, for example, describe plastic yielding induced by the crack or the accumulation of damage and the reduction of the material's compliance [34,35]. Such laws are challenged if one considers the behavior of individual samples, whose life-times usually vary considerably in nominally similar tests. The origins of this breakdown lie in the intermittency of the crack growth. The sample failure proceeds by avalanches of very different sizes (crack-length increments), with a cutoff expected to increase or possibly even diverge as the life time of the material is approached. Thus the randomness is even more pronounced than the nominal sample-to-sample variations of static strength and critical-crack size l_c would suggest. The important question we study here is from which point in time ("tipping point") is it possible guess or "forecast" the sample life-time in advance. We consider this first by monitoring the fracture by acoustic emission (AE) and then by an optical speckle technique that looks at the expansion of the crack and the process zone. In the experiments we perform, the question becomes how well

*mikko.alava@aalto.fi

these two techniques can be tuned to give an optimal level of predictability.

II. EXPERIMENTS

Paper samples of ordinary copy paper are prepared with sample dimensions of 100 mm (length and width). A precut edge notch is made on each sample with a 10-mm nominal length. The creep loading is applied by an Instron Electropuls E1000 tensile testing machine with a load ramp-up time of 10 s. The load level (46 N) is pretested so that the typical empirical lifetimes t_c will end up inside a time window of 100 to 1000 s. Due to the broad distribution of t_c [33], some samples do not fail and are discarded. The data from each test consist of the sample deformation vs time and AE data to follow the microcracking. The last available deformation point is used to define t_c. AE is detected with a piezoelectric transducer, which is attached to the sample. The AE events in notched-paper samples originate from the proximity of the fracture process zone to a notch and their localization is thus very difficult to do on a small scale and rather irrelevant on a large scale (above 1 mm). The sampling frequency is 1 MHz, and after thresholding, events are formed from data (see also Ref. [26]). From the data, event occurrence times t_i and energies E_i are extracted to form an AE event time series. The number of events in a time interval divided by the length defines the event rate $r(t)$. Each sample typically produces on the order of 10^3 events with the event definition (thresholding) used here. We present results from 26 experiments. We also perform an independent set of optical speckle measurements (see Sec. III C for details).

III. RESULTS

A. Sample creep response

Figure 1(a) shows the samples' behaviors by the strain rate ϵ_t for the set of experiments. At early stages (up to 10 s), the loading phase may be noticed. This is followed by a decaying-strain rate in analogy to the Andrade primary creep (power-law behavior $\epsilon_t \sim t^{-\alpha}$ with $\alpha \simeq 0.8$). Finally, at a sample dependent cross-over time $t_{\min}$, the creep rate reaches a minimum and then starts to increase, as happens in the creep failure of samples without notches [33]. Figure 1(b) shows the relation between the minimum strain rate time $t_{\min}$ and the life time t_c on a sample to sample basis. It is clear that only a weak linear correlation exists, and this is emphasized even more by the direct linear fit of the t_c as a function of $t_{\min}$. The lack of predictability from strain rate curves is also clear considering the variations of the inset. Figure 1(b) also shows error estimates for $t_{\min}$ originating from the noisiness of the data and the presence of "secondary minima," as one can see both in Fig. 1(a) and in more detail in its inset (Exp. 2 is an example).

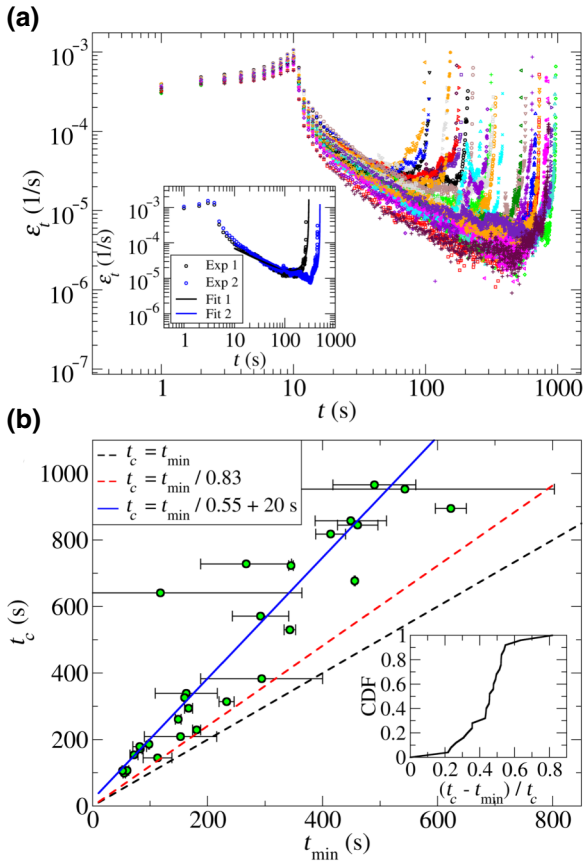

FIG. 1. (a) The strain rates ϵ_t measured in the experiments. Inset: two experiments and fits of the effective medium model to the same. (b) The failure time t_c vs the time of the minimum-strain rate $t_{\min}$. Two candidate scalings for a t_c proportional to $t_{\min}$ are indicated. Inset: the cumulative distribution function (CDF) of the relative difference $(t_c - t_{\min})/t_c$ of the failure time to the time at which the minimum-strain rate occurs.

Figure 2 illustrates from one sample in more detail the behavior of the sample strain rate ϵ_t. The presence of fluctuations is obvious, making among others the determination of the time of the minimum strain rate $t_{\min}$ [33] somewhat ambiguous. To account for the general features of the sample-level behavior, we constructed a model of a sample following in creep bulk Andrade rheology ($\epsilon_t \sim t^{-0.8}$ as found empirically [36]) in series with the crack propagation zone, whose elastic compliance decreases with the crack growth. The total sample deformation is given by the weighted average of the two creep deformation dynamics, of which comes from the faster and faster deformation of the crack propagation zone and the other one resulting from the decaying Andrade primary creep in the rest of the sample. The justification for this mean-field-like model comes from the fact that in the absence of noticeable crack growth, in the beginning of the experiments, the samples follow a version of typical

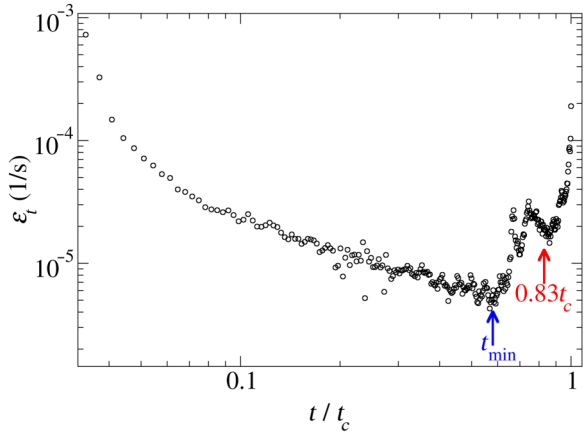

FIG. 2. An example of a strain rate ϵ_t as a function of scaled time t/t_c. The global minimum occurs at around $0.6t_c$, with a local minimum close to $0.83t_c$

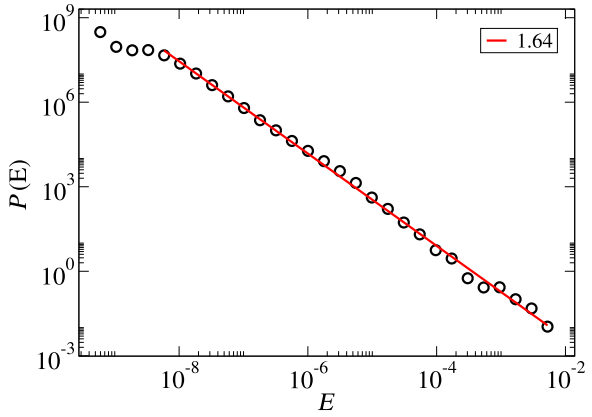

FIG. 4. The probability density function of event energies for 26 experiments. A power law, $P(E) \sim E^{-\tau_E}$ with $\tau_E \approx 1.6$, fits the data well.

Andrade primary creep, and later this must be of secondary importance due to the creep growth of the crack.

We show in Fig. 3(a) a comparison of four cases, where the growth law for the crack $L(t) = L_0 + \Delta L(t)$ (L_0 is the initial notch size and ΔL the increment) is either polynomial (second order in time), exponential, or is exponential in time for the increment. Another possibility in analogy with Santucci *et al.* for paper samples [24] is $\Delta L = \xi \log(1 - t/\tau)$, which allows to search for fits to sample-dependent behavior, including t_c, by changing the crack-growth scale ξ and timescale τ, in addition to the relative amplitudes of Andrade and crack-zone dynamics. We observe that the two latter procedures produce roughly similar dynamics, and we use the last one for the two qualitative fits presented in the inset of Fig. 1(a) for two individual experiments.

These fits and the actual strain response ϵ_t of individual samples imply that establishing the lifetime from such macroscopic signatures will not work. Figure 1(b) illustrates this with a comparison of $t_{\min}$ to the lifetime t_c: the sample-to-sample variation of t_c is large. The quantity $t_{\min}$ is not easy to establish nor is it a good predictor of t_c (the inset of Fig. 1(b) shows that the cumulative relative difference between t_c and $t_{\min}$ is substantial). After considering the sample creep response, we are left with the question, to which degree can the lifetime be predicted based on quantities that are derived from the growth dynamics of the crack itself?

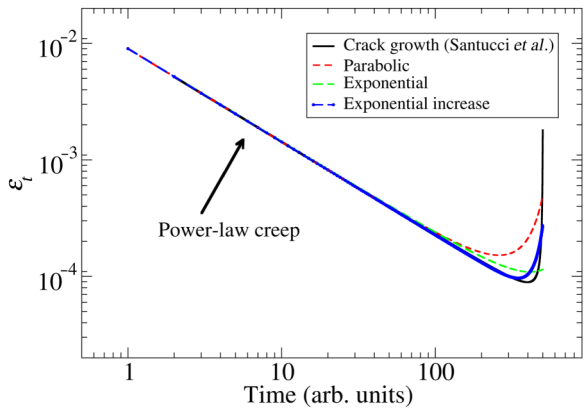

FIG. 3. An example of four different models for the crack-growth dynamics together with a power-law bulk creep response and the resulting specimen response.

B. Acoustic emission

For any experiment, AE measurement provides a method for following the fracture dynamics with high temporal resolution, in particular, compared to optical means [26,37–41]. For background information and as a check, we compute the histogram of the AE event energies $P(E)$ (Fig. 4). This appears, in analogy to most other AE energy distributions, in particular for paper, to have a power-law shape with an exponent in qualitative and quantitative agreement with earlier paper data [26,37].

The integrated number of events $N(t)$ and integrated energy $E(t)$ both clearly exhibit sample-to-sample variation and show the randomness of crack growth (Fig. 5). Both $N(t)$ and $E(t)$ increase faster and faster with time. In an experiment, as t_c is approached in time, a crucial question is whether the actual data show signatures of divergence as a function of $t_c - t$ [18,19,23,25,26,29,31,32] such as $E(t) \propto (t_c - t)^{-a}$, where a is an empirical exponent for the divergence. For avalanching processes, this will be the case if the energy scale and/or the waiting time scales—the cutoffs of the event energy distribution $P(E_i)$ or the waiting time distribution—will cause this. The essence of being able to find such a divergence is that a sample would "know" its lifetime in a way that would allow determining it in advance from the sample behavior.

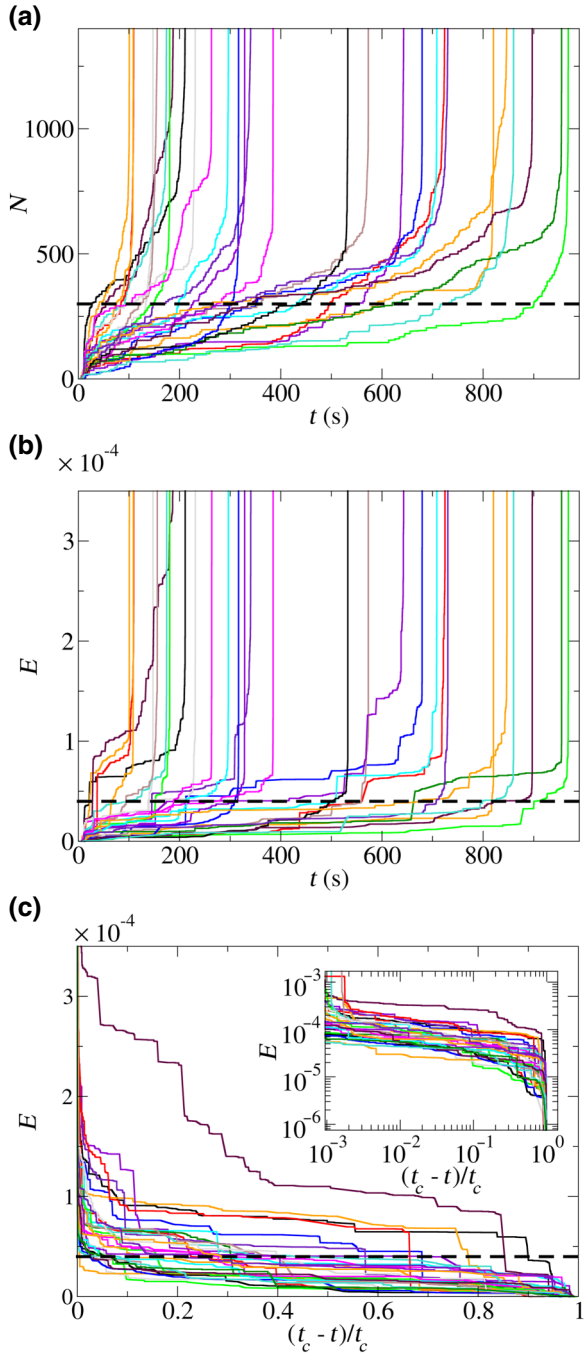

FIG. 5. (a) AE events $[N(t)]$ over the creep experiment. (b) AE energy $E(t)$ [in arb. units] over the experiments. (c) The same data collapsed using t_c to scale the experiment (inset in log-log scale). In all the subfigures, the main prediction threshold used later is indicated.

To select trial criteria for t_c prediction also means, in principle, having to make compromises. This comes in part from the inherent contradiction of having (possibly) predictability and it being useful (done "early"), and it in part results from the fluctuating nature of the $E(t)$-time series. Figure 6 shows that this in the case for event number $N(t)$

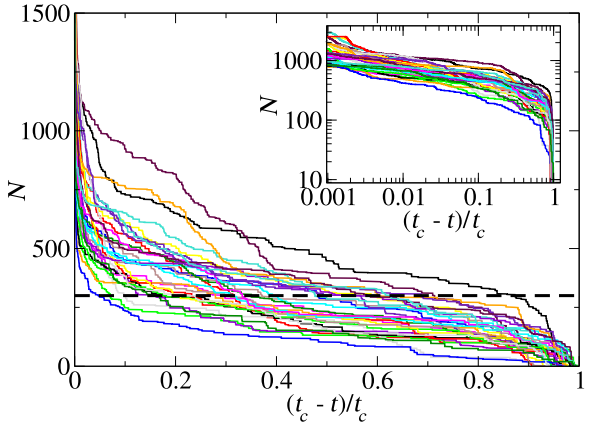

FIG. 6. Number of AE events N as a function of time scaled by the sample lifetime. The dashed line indicates a threshold of $N_{\mathrm{thr}} = 300$. The inset shows the data on a log-log scale.

and illustrates why $N_{\mathrm{thr}} = 300$ is chosen; we return to this question (what threshold is too low, what too high?) below. Another attractive idea is to use the energy or event rate as a warning signal ("rate exceeds a threshold for the first time indicates a precursor, which can be used to forecast sample failure"). Figure 7 shows that this is not a working idea. This is because even though the average rate has an increasing trend in individual experiments, there are large variations of the rates over the course of the lifetime of any particular sample. Figure 8 furthermore shows that the total AE energy detected and the largest event energy are not strongly correlated with t_c.

Clearly, neither of the two statistics, E (Fig. 5(c) nor $N(t)$, is a good candidate for this kind of divergence to be present. For integrated energy, this would result, for instance, if the crack length increment diverged upon approach to t_c, causing an increase in the cutoff of the corresponding AE event sizes. The interpretation of the data shown here is that there is no sign of such a critical divergence, which can be used to predict t_c. The divergence would mean being able to fit each sample with an envelope curve utilizing a power-law divergence to the data (N

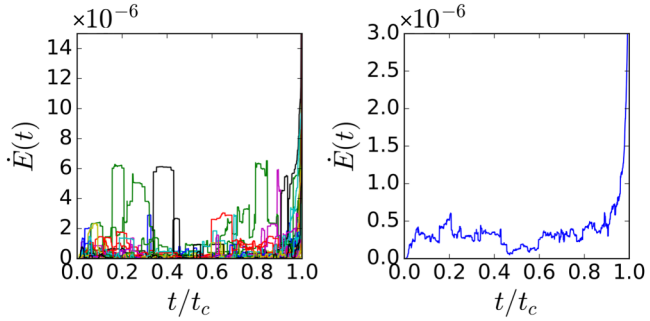

FIG. 7. Energy rates as a function of scaled time. Left panel: individual experiments. Right panel: average.

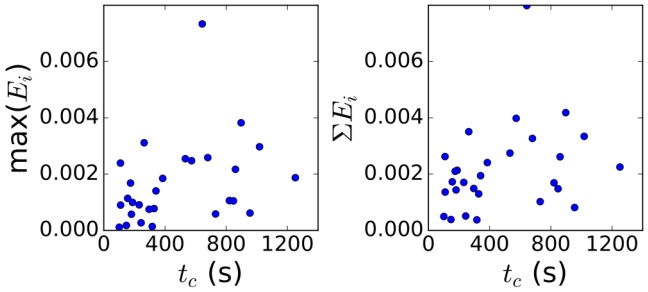

FIG. 8. Left panel: scatter plot of the sample lifetime and energy of the largest event. Right panel: scatter plot of lifetime vs total acoustic energy during the entire experiment.

or E) as a function of $t_c - t$ and extracting an estimate for t_c well in advance.

As a precursor, one might consider looking at the first occurrence of particularly high event rates [42], but this suffers from the same problem as the sample macroscopic strain rate: large variations exist through the duration of an experiment without any clear correlation to t_c. Another approach is to look at threshold quantities that may be connected to the first signs of accelerating crack growth or an increase of crack length l. Two candidates for this are the accumulated number of AE events $N(t)$ and the integrated AE energy $E(t)$ [39,43]. In other words, the question is whether the total number of avalanches or the energy released in crack advancement are useful predictors of t_c.

Figure 9 shows the result of an attempt to use a threshold of $N = 200{-}400$ for defining a threshold time $t_{\mathrm{thr},N}$ [for the choice of these particular threshold values, cf. Fig. 5(a)]. The N is chosen to have an early warning threshold. The resulting $t_{\mathrm{thr},N}$ are not very informative about t_c, as is shown in Fig. 9(b) with the CDF of the difference between the failure time and the threshold time. The opposite will be the case if t_c has a clear functional dependence on t_{thr}, for example, via a constant offset or being linearly proportional, $t_c \propto t_{\mathrm{thr}}$. For the smallest N, we clearly see that the predictability is quite low, whereas for the highest N (400), the failure time is obviously rather close to the threshold time. We argue that the intermediate value is a compromise. One should note that this trend is a generic one in prediction schemes based on thresholds and applies both to N and $E(t)$ alike. An a posteriori normalization of the "error" with t_c (CDFs shown in the insets) seems to indicate, the failure time and the threshold time are related by a power-law relationship, which depends on N.

An analogous analysis for $E(t)$ using threshold energy $E(t) = 4 \times 10^{-5}$ is presented in Fig. 9(g). Again, the threshold value is chosen to try to predict an early t_c, if possible. The correlation in this case is slightly better than in the case of "N." Repeating the analysis of $t_c - t_{\mathrm{thr}}$

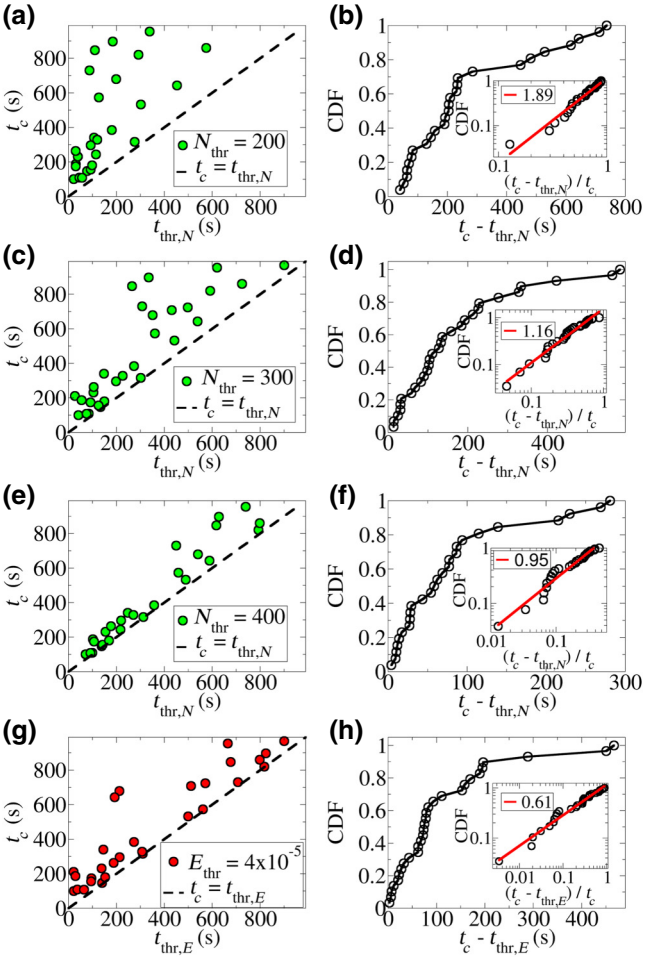

FIG. 9. (a),(c),(e) Failure time t_c vs threshold time $t_{\mathrm{thr},N}$ for three event-number thresholds, $N = 200$, 300, and 400. (b),(d),(f) The CDF of the difference $t_c - t_{\mathrm{thr},N}$ for the same data. The inset shows the CDF of the data normalized case by case by t_c. (g) The prediction from $t_{\mathrm{thr},E}$ in analogy to the case of N. Threshold energy $E = 4 \times 10^{-5}$ [arb. units]. (h) The same data as in (b) to (f).

[Fig. 9(h) and inset] demonstrates this. Again, we discover that the relative errors have a CDF with a power-law scaling in the limit of small errors. All in all, trying to find thresholds from the crackling noise of early to intermediate times does not result in a good predictor of t_c. The AE energy, taken as a measure of the crack propagation (crack length), works slightly better than the number of detected "crack tip jumps" or AE events (however, see Ref. [31]).

C. Fracture process zone and speckle pattern analysis

We perform speckle analysis of dynamics around the crack tip in order to determine the point at which crack propagation might become predictable due to fracture process zone (FPZ) growth. The speckle technique works with

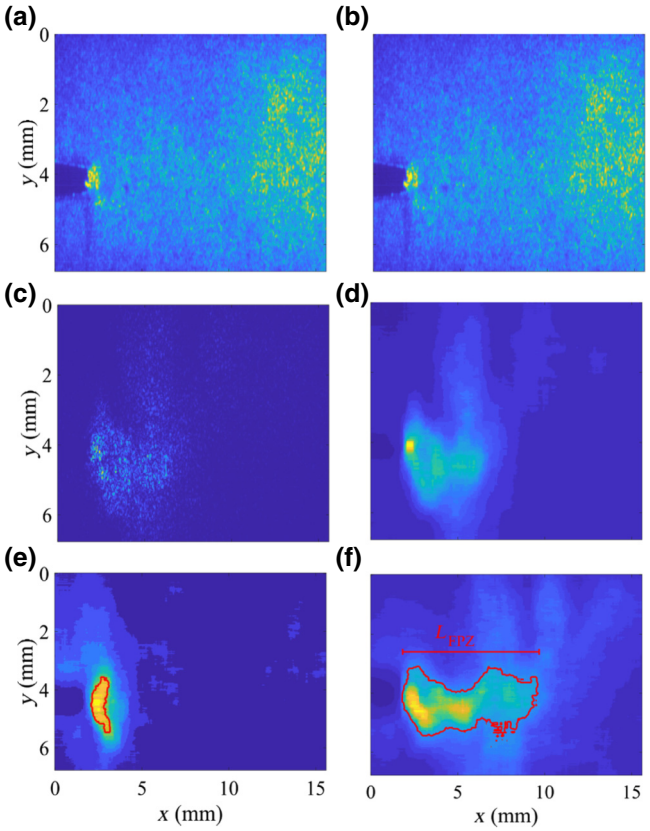

FIG. 10. (a),(b) Speckle patterns at two different times (20 ms delay). (c) Related change. (d) Pattern after filtering. (e) Speckle determination of the process zone at approximately 0.3 t_c (for this sample) and (f) at 0.8 t_c. The color code measures the intensity of the transmitted light [(a),(b)] or the local surface deformation activity from low (blue) to high (yellow) [(c)–(f)].

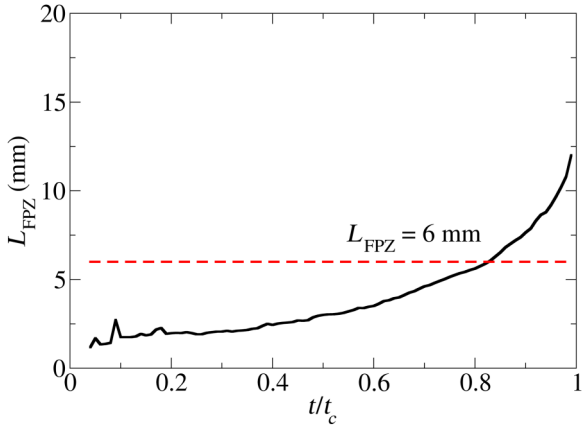

FIG. 11. Average process zone length as a function of scaled time.

a fast (but not comparable to AE) time resolution. Measurements with an image frequency of 500 Hz and less than 100 s length (for device memory reasons) are carried out. Simultaneous AE measurements are done with a resolution of 460 × 200 pixels, leading to an image area of 15.64 mm × 6.80 mm^2 focused at the crack. Each pixel is measured on a brightness scale from 0 to 255. Due to a memory limited measurement time, the experimental conditions are changed so that the typical durations and AE event counts become smaller. The FPZ is calculated by comparing two speckle pattern images that are separated by 20 ms [Figs. 10(a) and 10(b)]. Both are 8-bit gray-scale images. The difference of the images is calculated by subtracting one from the other pixelwise and taking the absolute values [Fig. 10(c)]. Next, the difference image is smoothed using median filtering over an area of 25 × 25 pixels. First, each pixel (i,j) is replaced by the median over the pixels $[(i-12,j),(i+12,j)]$. Then this pixel is replaced by the median in the other direction over the pixels $[(i,j-12),(i,j+12)]$. The smoothed image is shown in Fig. 10(d). A FPZ is defined by thresholding the pixel values. The length of the resulting process zone (L_{FPZ}) can then be extracted in the crack growth direction. Figure 10 illustrates the measure with scale bars and the corresponding process zones. In other words, this technique looks at the short-time changes in the surface topography of the samples. The process zone in paper is traditionally measured by a-posteriori techniques [44] and dissipated energy in the fracture is also visible with IR imaging [45]. The process zone plays a similar role as in the general fracture of heterogeneous media [46,47], and is an important quantity for the material fracture toughness and strength.

Figure 11 demonstrates the growth of L_{FPZ} as extracted by the speckle method in scaled time units (with t_c). The figure serves to justify the choice of the simple scale of 6 mm for L_{FPZ}. A larger value would mean that the ratio of the predicted t_c and the threshold time would be quite close to unity, and decreasing the value would start to increase the scatter or the difference of the predicted and actual t_c. This particular value for the threshold process zone size is quite large. The typical growth of L_{FPZ} accelerates again with time, with noticeable sample-to-sample variations and some intermittency. Part of such fluctuations, in particular at the early stages of the crack growth, result from the indirect nature of the speckle analysis method. Figure 12(a) shows that the AE data [here, we use $N(t)$] are proportional to L_{FPZ} with a "prefactor" that depends on the sample. A similar "early time warning analysis" is performed for N and E. This yields the result shown in Fig. 12, with $L_{FPZ} = 6$ mm. Note that the measured L_{FPZ} does not differentiate well between crack growth $L(t)$ and the growth dynamics of the process zone in front of the actual crack. This result means (as confirmed by the CDF shown in Fig. 12(c) that there is a strong correlation of individual pairs of values of t_c and $t_{thr,FPZ}$ and the relationship is quite close to linear, with $t_c \propto 1.25\, t_{thr,FPZ}$.

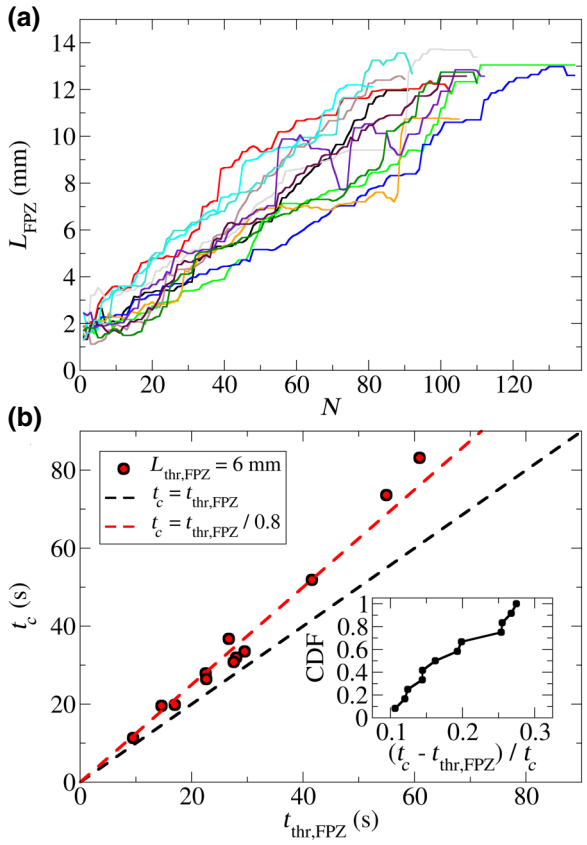

FIG. 12. (a) L_{FPZ} vs N. (b) Failure time t_c vs threshold time $t_{thr,FPZ}$ for a process zone length threshold, $L_{FPZ} = 6$ mm. Inset: the CDF of the difference, $t_c - t_{thr,FPZ}$, for the same data.

IV. CONCLUSIONS

Predicting the lifetime of a sample when a crack grows in creep conditions is inherently difficult since the crack dynamics is intermittent. The question is whether the bursty avalanches and their history in a sample can be used to predict when that particular will reach its lifetime. One candidate for this is the approach "to a critical point," which means again that the behavior of a measured quantity will exhibit a regular behavior as a function of the difference $t_c - t$ in each sample, which, in turn, might be used to fit the data to extract t_c in advance. What we find experimentally is that macroscopic sample behaviors exhibit individual creep responses characterizing a U-shaped creep rate in time, with a creep rate minimum reached at a related time t_{min}. The ratio t_{min}/t_c shows large variations, and this results in sample-dependent microscopic detail, which, in general, makes t_c-prediction attempts futile, at least until t_{min} if not beyond.

The crack growth is easy to monitor with great temporal accuracy with AE detection, and whether the stochastic AE signal can be used to yield useful indicators or reliable early warning signatures to predict t_c turns out to have a negative answer. The reason for this lies in the fact that in a material with a sizable process zone, the development of the integrated AE can not be summarized in an envelope curve which can be "parameterized," as above, or fitted with a few parameters such as t_{min}, t_c from data well before t_c and then used to predict t_c in advance. This is so as regards any divergences approaching the t_c of a sample, but the idea should be tested again in quasi-brittle materials, in particular when one expects crack growth dynamics to be governed by a depinning transition [43,48,49].

The use of optical speckle analyses shows that at later stages, monitoring both the growth of the crack and the process zone results in a length scale. This works as a threshold quantity that correlates well with the lifetime, but the procedure is of little general applicability compared to AE-based passive observation methods. A similar approach can also be attempted by using AE localization methods, but since we are looking at near-crack-tip phenomena, this is quite difficult—it is challenging to locate events with a spatial accuracy comparable to the speckle approach. One can predict failure not by listening, but by looking at its growth. This result does not bode well for the indirect monitoring of sample or structural failure using the AE technique, in general. However, other scenarios may be easier. The case of quasi-brittle materials is mentioned and another case would be when the lifetime is determined by the stochastic nucleation of a micro- or meso-scale crack and its subsequent propagation, which might be amenable to AE detection and/or localization, in particular, if the critical crack size is "large."

ACKNOWLEDGMENTS

We acknowledge the financial support of the Academy of Finland through the COMP Center of Excellence (Grant No. 251748).

[1] D. Bonamy and E. Bouchaud, Failure of heterogeneous materials: A dynamic phase transition? Phys. Rep. **498**, 1 (2011).
[2] M. Alava, P. K. Nukala, and S. Zapperi, Statistical models of fracture, Adv. Phys. **55**, 349 (2006).
[3] J. P. Sethna, K. A. Dahmen, and C. R. Myers, Crackling noise, Nature **410**, 242 (2001).
[4] K. J. Måløy, S. Santucci, J. Schmittbuhl, and R. Toussaint, Local Waiting Time Fluctuations Along a Randomly Pinned Crack Front, Phys. Rev. Lett. **96**, 045501 (2006).
[5] D. Bonamy, S. Santucci, and L. Ponson, Crackling Dynamics in Material Failure as the Signature of a Self-Organized Dynamic Phase Transition, Phys. Rev. Lett. **101**, 045501 (2008).
[6] S. Janićević, L. Laurson, K. J. Måløy, S. Santucci, and M. J. Alava, Crackling Dynamics in Material Failure as the Signature of a Self-organized Dynamic Phase Transition, Phys. Rev. Lett. **117**, 230601 (2016).

[7] I. G. Main, A damage mechanics model for power-law creep and earthquake aftershock and foreshock sequences, Geophys. J. Int. **142**, 151 (2000).
[8] V. Keilis-Borok, Earthquake prediction: State-of-the-art and emerging possibilities, Annu. Rev. Earth Planet. Sci. **30**, 1 (2002).
[9] M. C. Gerstenberger, S. Wiemer, L. M. Jones, and P. A. Reasenberg, Real-time forecasts of tomorrow's earthquakes in California, Nature **435**, 328 (2005).
[10] V. G. Kossobokov, Testing earthquake prediction methods: "The West Pacific short-term forecast of earthquakes with magnitude MwHRV $\geq$ 5.8", Tectonophysics **413**, 25 (2006).
[11] A. F. Bell, M. Naylor, M. J. Heap, and I. G. Main, Forecasting volcanic eruptions and other material failure phenomena: An evaluation of the failure forecast method, Geophys. Res. Lett. **38**, L15304 (2011).
[12] T. Jordan, Y. Chen, P. Gasparini, R. Madariaga, I. Main, W. Marzocchi, G. Papadopoulos, G. Sobolev, K. Yamaoka, and J. Zschau, Operational earthquake forecasting: State of knowledge and guidelines for utilization, Ann. Geophys. **54**, 315 (2011).
[13] A. F. Bell, M. Naylor, and I. G. Main, The limits of predictability of volcanic eruptions from accelerating rates of earthquakes, Geophys. J. Int. **194**, 1541 (2013).
[14] S.-W. Hao, B.-J. Zhang, J.-F. Tian, and D. Elsworth, Predicting time to failure in rock extrapolated from secondary creep, J. Geophys. Res. **119**, 1942 (2014).
[15] M. Rosenau, F. Corbi, and S. Dominguez, Analogue earthquakes and seismic cycles: Experimental modelling across timescales, Solid Earth **8**, 597 (2017).
[16] N. Brantut, M. J. Heap, P. G. Meredith, and P. Baud, Time-dependent cracking and brittle creep in crustal rocks: A review, J. Struct. Geol. **52**, 17 (2013).
[17] B. Voight, A relation to describe rate-dependent material failure, Science **243**, 200 (1989).
[18] A. Guarino, A. Garcimartin, and S. Ciliberto, An experimental test of the critical behaviour of fracture precursors, Eur. Phys. J. B **6**, 132 (1998).
[19] D. Sornette, Predictability of catastrophic events: Material rupture, earthquakes, turbulence, financial crashes, and human birth, PNAS **99**, 2522 (2002).
[20] A. Guarino, S. Ciliberto, A. Garcimartin, M. Zei, and R. Scorretti, Failure time and critical behaviour of fracture precursors in heterogeneous materials, Eur. Phys. J. B **26**, 141 (2002).
[21] R. C. Hidalgo, F. Kun, and H. J. Herrmann, Creep rupture of viscoelastic fiber bundles, Phys. Rev. E **65**, 032502 (2002).
[22] S. Santucci, L. Vanel, and S. Ciliberto, Sub-critical Statistics in Rupture of Fibrous Materials: Model and Experiments, Phys. Rev. Lett. **93**, 095505 (2004).
[23] H. Nechad, A. Helmstetter, R. El Guerjouma, and D. Sornette, Creep Ruptures in Heterogeneous Materials, Phys. Rev. Lett. **94**, 045501 (2005).
[24] S. Santucci, P.-P. Cortet, S. Deschanel, L. Vanel, and S. Ciliberto, Subcritical crack growth in fibrous materials, Europhys. Lett. **74**, 595 (2006).
[25] L. Girard, D. Amitrano, and J. Weiss, Failure as a critical phenomenon in a progressive damage model, J. Stat. Mech. **2010**, P01013 (2010).
[26] J. Rosti, J. Koivisto, and M. Alava, Statistics of acoustic emission in paper fracture: Precursors and criticality, J. Stat. Mech. **2010**, P02016 (2010).
[27] M. Leocmach, C. Perge, T. Divoux, and S. Manneville, Creep and Fracture of a Protein Gel under Stress, Phys. Rev. Lett. **113**, 038303 (2014).
[28] T. H. Dixon, Y. Jiang, R. Malservisi, R. McCaffrey, N. Voss, M. Protti, and V. Gonzalez, Earthquake and tsunami forecasts: Relation of slow slip events to subsequent earthquake rupture, PNAS **111**, 17039 (2014).
[29] G. F. Nataf, P. O. Castillo-Villa, P. Sellappan, W. M. Kriven, E. Vives, A. Planes, and E. K. H. Salje, Predicting failure: Acoustic emission of berlinite under compression, J. Phys.: Condens. Matter **26**, 275401 (2014).
[30] F. Kun, I. Varga, S. Lennartz-Sassinek, and I. G. Main, Rupture Cascades in a Discrete Element Model of a Porous Sedimentary Rock, Phys. Rev. Lett. **112**, 065501 (2014).
[31] S. Lennartz-Sassinek, I. G. Main, M. Zaiser, and C. C. Graham, Acceleration and localization of subcritical crack growth in a natural composite material, Phys. Rev. **E90**, 052401 (2014).
[32] J. Vasseur, F. B. Wadsworth, Y. Lavallée, A. F. Bell, I. G. Main, and D. B. Dingwell, Heterogeneity: The key to failure forecasting, Sci. Rep. **5**, 13259 (2015).
[33] J. Koivisto, M. Ovaska, A. Miksic, L. Laurson, and M. J. Alava, Predicting sample lifetimes in creep fracture of heterogeneous materials, Phys. Rev. **E94**, 023002 (2016).
[34] K. M. Nikbin, D. J. Smith, and G. A. Webster, An engineering approach to the prediction of creep crack growth, J. Eng. Mat. Techn. **108**, 186 (1986).
[35] J. L. Chaboche, Continuum damage mechanics: Part II Damage growth, crack initiation, and crack growth, J. App. Mech. **55**, 65 (1988).
[36] J. Rosti, J. Koivisto, L. Laurson, and M. J. Alava, Fluctuations and Scaling in Creep Deformation, Phys. Rev. Lett. **105**, 100601 (2010).
[37] L. I. Salminen, A. I. Tolvanen, and M. J. Alava, Acoustic Emission from Paper Fracture, Phys. Rev. Lett. **89**, 185503 (2002).
[38] J. Davidsen, S. Stanchits, and G. Dresen, Scaling and Universality in Rock Freacture, Phys. Rev. Lett. **98**, 125502 (2007).
[39] M. Stoljanova, S. Santucci, L. Vanel, and O. Ramos, High Frequency Monitoring Reveals Aftershocks in Subcritical Crack Growth, Phys. Rev. Lett. **112**, 115502 (2014).
[40] S. Deschanel, L. Vanel, N. Godin, G. Vigier, and S. Ciliberto, Experimental study of crackling noise: conditions on power law scaling correlated with fracture precursors, J. Stat. Mech. **2009**, P01018 (2009).
[41] A. Tantot, S. Santucci, O. Ramos, S. Deschanel, M.-A. Verdier, E. Mony, Y. Wei, S. Ciliberto, L. Vanel, and P. C. F. Di Stefano, Sound and Light from Fractures in Scintillators, Phys. Rev. Lett. **111**, 154301 (2013).
[42] J. Baro, A. Corral, X. Illa, A. Planes, E. K. H. Salje, W. Schranz, D. E. Soto-Parra, and E. Vives, Statistical Similarity between the Compression of a Porous Material and Earthquakes, Phys. Rev. Lett. **110**, 088702 (2013).

[43] J. Bares, M. L. Hattali, D. Dalmas, and D. Bonamy, Fluctuations of Global Energy Release and Crackling in Nominally Brittle Heterogeneous Fracture, Phys. Rev. Lett. **113**, 264301 (2014).

[44] M. J. Alava and K. J. Niskanen, The physics of paper, Rep. Prog. Phys. **69**, 669 (2006).

[45] R. Toussaint, O. Lengliné, S. Santucci, T. Vincent-Dospital, M. Naert-Guillot, and K. J. Måløy, How cracks are hot and cool: A burning issue for paper, Soft Matter **12**, 5563 (2016).

[46] Z. P. Bazant, Scaling theory for quasibrittle structural failure, PNAS **101**, 13400 (2004).

[47] M. J. Alava, P. K. Nukala, and S. Zapperi, Role of Disorder in the Size Scaling of Material Strength, Phys. Rev. Lett. **100**, 0555502 (2008).

[48] K. T. Tallakstad, R. Toussaint, S. Santucci, J. Schmittbuhl, and K. J. Måløy, Local dynamics of a randomly pinned crack front, Phys. Rev. **E83**, 046108 (2011).

[49] J. Bares, A. Dubois, L. Hattali, D. Dalmas, and D. Bonamy, Aftershock sequences and seismic-like organization of acoustic events produced by a single propagating crack, Nat. Comm. **9**, 1253 (2018).